Use of a High Resolution Overview Spectrometer for the Visible Range in the TEXTOR Boundary Plasma

Sebastijan Brezinsek, Albrecht Pospieszczyk, Gennadij Sergienko, Phillipe Mertens, Ulrich Samm

Institut für Energieforschung - Plasmaphysik, Forschungszentrum Jülich GmbH
EURATOM-Association, Trilateral Euregio Cluster, D-52425 Jülich, Germany

October 22, 2007

Passive spectroscopy is a standard diagnostic to observe the boundary layer of fusion plasmas. This visible spectroscopy is focused on the measurement of the deuterium recycling flux as well as on the monitoring of impurity fluxes like e.g. O, He... or W, C... which result from erosion of plasma-facing components. Moreover, the ro-vibrational analysis of molecular transitions provide information about the molecular break-up in the plasma. Spectrometer for the plasma boundary have to fulfil high demands with respect to the spectral, spatial and time resolution, to the observable wavelength range, to the sensitivity and dynamic range of the detector to observe and analyse simultaneously the emission of atomic and molecular species present in the observed region. We present an overview spectrometer system which is able a) to measure at once strong atomic lines (e.g. D_α) and weak molecular bands (e.g. C_2 Swan-band), b) to resolve narrow molecular lines (e.g. D_2 Fulcher-α band) and allow their ro-vibrational analysis, and c) to provide information about the spatial distribution in the plasma boundary. A full characterisation of the custom-made system in cross-dispersion arrangement with respect to resolving power, simultaneous wavelength coverage, sensitivity etc. is done. Spectra examples ("footprints") taken from an injection of C_3H_4 into TEXTOR are presented.

Keywords: Plasma-Wall Interaction, Cross-Dispersion Spectrometer, Plasma Boundary Spectroscopy, Fulcher-α band Spectroscopy, Hydrocarbon Break-Up Mechanism

1 Introduction

Present-day fusion devices use graphite and/or tungsten as a plasma-facing material (PFM) at the locations of highest particle flux such as the divertor target plates. Complex processes such as physical and, in the case of graphite, chemical sputtering take place at the surface. Material erosion and subsequent deposition leads to the formation of surface layers, which can -in the presence of two or more PFMs- contain complex mixed materials. A limited number of *in situ* diagnostics is currently available to identify and monitor the different species which are released from these PFMs under particle bombardment.

Passive spectroscopy in the visible range is a standard diagnostic to monitor the fluxes of carbon-containing species (C, CD...), which are released from the surface or build during the molecular break-up [1], other fusion-plasma related impurities (W, O...) as well as the fluxes of recycled fuel particles (D, D_2...). To observe and analyse the emission of these species simultaneously from a given observation volume, a spectrometer system has to fulfil high demands with respect to the spectral, spatial and time resolution, to the observable wavelength range, to the sensitivity and dynamic range of the detector. An optimised system should be able a) to measure at once strong atomic lines (e.g. D_α) and weak molecular bands (e.g. C_2 Swan-band), b) to resolve narrow molecular lines (e.g. D_2 Fulcher-α

band) and allow their ro-vibrational analysis, and c) to provide information about the spatial distribution.

We present and characterise a spectrometer in cross-dispersion arrangement which can be applied as good compromise and which fulfils most of the needs apart from the spatial distribution from a single measurement. Experiments with injection of C_3H_4 were carried out in TEXTOR and spectra of the break-up products such as CH and C_2 were recorded simultaneously to demonstrate the potential of the device. Moreover the D_2 Fulcher-α was observed during local D_2 injection and ro-vibrationally analysed.

2 The cross-dispersion spectrometer – principle function, set-up and technical data

Conventional spectrometers, e.g. in Czerny-Turner ar-
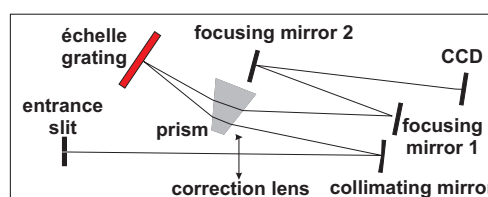
Fig. 1   Schematic view of the spectrometer set-up.

rangement, are equipped with only *one* dispersive element: grating or prism. Single dispersion systems are restricted

in the simultaneously covered wavelength span to a few nanometres at a typical resolving power $R = \lambda/\Delta\lambda$ of 20,000 which is mandatory for a ro-vibrational analysis of molecular transitions. The most prominent D_2 transition in fusion boundary plasmas - the Fulcher-α band - is spread over a wide spectral range (600 nm - 645 nm), thus, several discharges are necessary to record the full spectrum which is needed for spectral analysis.

In contrast, the custom-made spectrometer presented here (MI, model: Mechelle 7500 special; schematic set-up in fig. 1) consists of *two* dispersive elements: prism and grating. The system covers a spectral range of more than 300 nm without gap with the requested high spectral resolution. The wide span is achieved though the combined use of (i) a highly dispersive échelle grating (ruling: 31.6 grooves/mm, size 10.0 cm × 3.0 cm, blaze angle 63.5°) for wavelength dispersion in horizontal direction and (ii) an order sorter, a highly dispersive prism (BAF50 glass, reference angle 36°), which separates the orders in vertical direction. The prism is used twice in the optical path (fig. 1) to ensure complete order separation with compact prism size.

Fig. 2a shows the observable spectral orders m projected on the CCD array, starting from $m=153$ at the bottom (blue spectral range) to $m=79$ on the top (red spectral range), as well as the used spectral range in each order which is applied for the spectrum reconstruction. The centre wavelength in each order, positioned at the blaze angle of the grating, is determined by the order constant $m \times \lambda[\mu m]$ which amounts to 56.783 for this system. The overlap of different orders is determined by the condition $\frac{m=x+0.5}{56.783} = \lambda_{min}^{m=x} = \lambda_{max}^{m=x+1}$ while five additional pixels on each side are used for averaging. Fig. 2b shows the contribution of each order to the *standard range* between 372 nm ($m=152$) and 680 nm ($m=84$). The 92th order is in the next figures marked in red as guide for the eye. The spectrum in each order is spread across several pixels in vertical direction. Thus, a summation over 5 to 7 pixels is made to increase the sensitivity of the system and provides a so-called spectral channel. Additionally, the spectrum reconstruction [2] takes into account the non-equidistant separation of the channels, which are more compressed in the lower orders, as well as their curvature in the higher orders.

Fig. 2c depicts the linear dispersion as a function of the wavelength in the standard range. Although the dispersion varies over the full range, the resulting resolving power, which was measured by applying the Rayleigh criterium to pairs of D_2 lines, is within 15% almost constant at 20,000 when the apparatus function is considered. The latter was estimated by the line width of Hg lines, in particular of Hg*I* at 529 nm to be below 3.1 channel (FWHM) as shown in the Gaussian fit in fig. 2d.

Further technical data of the Mechelle are: aperture value $f/7$, focal length $f_L = 190$ mm, entrance slit 25 μm×75 μm with SMA905 connector for fibre coupling. Light is coupled to the system by means of 600 m quartz fibre. A 16
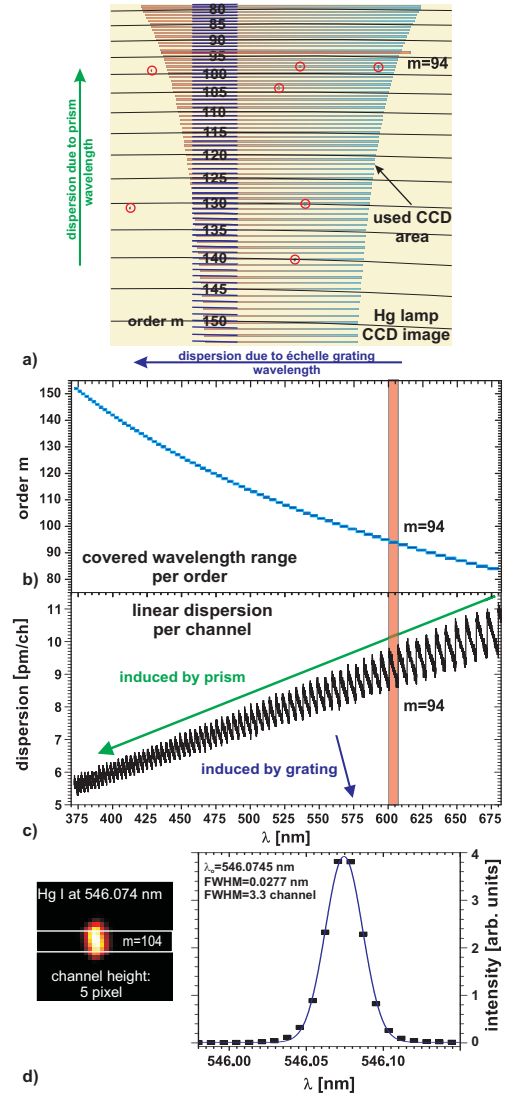
Fig. 2   Spectrum reconstruction: a) 2D image of a Hg line spectrum. The spectral range per order applied for the complete spectrum reconstruction is given by the envelope. b) Distribution of the wavelength coverage per order. c) The linear dispersion over the full spectral range. d) A Hg I line is used to approximate the apparatus function.

bit camera (Andor, model: DV434) with a Peltier-cooled back-illuminated CCD array, 1024×1024 pixels and 13 μm ×13 μm each pixel, is used as detector. The CCD has a broadband coating optimised for the visible range and provides a quantum efficiency of more than 90% at 500 nm and −60° C cooling temperature. The read-out time for the full frame amounts to one second at the maximum read-out frequency of 1 MHz.

3   Spectral and radiometric calibration

The spectral calibration is performed with the aid of a Hg lamp. The position of seven Hg*I* lines, marked in fig. 2a, is compared with theoretically calculated positions. The deviation between calculated and measured position is minimised in a least-square fit procedure. The overall position

precision lies within two spectral channels and shows almost no drift under controlled temperature conditions. An
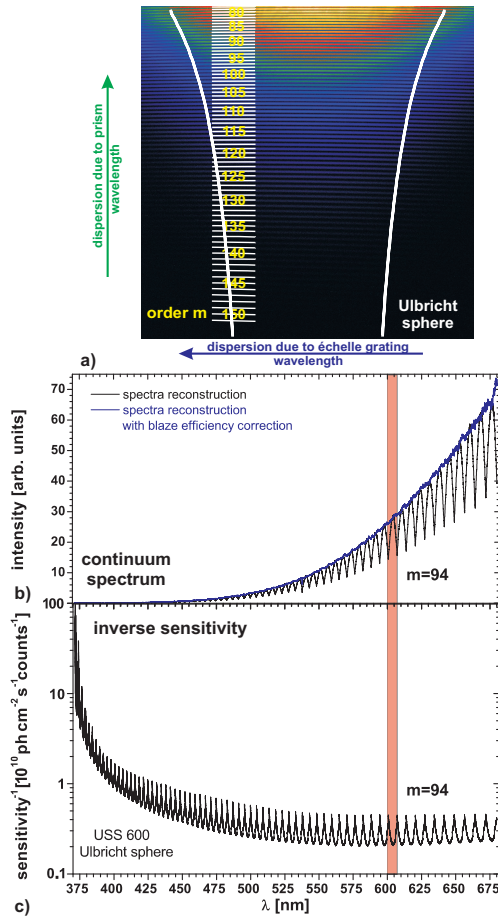
Fig. 3 Radiometric calibration of the cross-dispersion spectrometer. a) 2d image of the system during exposure by a continuum light source. b) Complete reconstructed spectrum of the continuum spectrum. Intensity drops caused by the blaze angle dependence of the grating are considered in the calibration by a correction function. c) The spectral response of the system for the full wavelength span.

Ulbricht sphere is used to calibrate the spectrometer system radiometrically. Fig. 3a shows a false-colour 2D image taken from the continuum source; the resulting reconstructed spectrum is depicted in fig. 3b. The spectrum is a convolution of the light source continuum and the sensitivity response of the detection system. Both image and spectrum show a non-uniformity of the measured radiation within each order. The reduction of the sensitivity of about 40% between the centre and the edges is caused by the blaze angle dependence of the grating. A correction function is introduced to compensate these strong sensitivity drops in the spectrum. The cross-talk between adjacent orders is measured to be below 10^{-3}, and any impact on the calibration can be neglected for the standard range.

The bare inverse sensitivity curve for the standard range is depicted in fig. 3c. The spectrometer system, which is optimised for the visible emission range according to the choice of prism, grating and CCD coating, shows an al-

most constant spectral response above 450 nm. However, the sensitivity drops significantly between 450 nm and 380 nm, which is largely caused by the reduction of the CCD quantum efficiency of about 50%, and by the decrease of the glass transmission from 95% to 55% due to 25 mm absorption length in the prism.

4 Spectra examples: hydrocarbon and deuterium molecules

A series of experiments with the injection of different hydrocarbon species (CH_4, C_3H_4 *etc.*) in similar plasmas has been started in TEXTOR. The aim of the experiments is a) to check if the injected stable hydrocarbon leaves a "footprint" e.g. with regard to its appearance, intensity ratio, ro-vibrational population of the break-up products C_2, CH, CH^+ *etc.*, and b) to determine the inverse photon efficiencies and branching ratios which relate the photon flux of the break-up products to the particle flux of injected species. An example of a "footprint" spectrum is depicted in fig. 4a. Spectra of the band heads of the most important transitions, CH Gerö-band and C_2 Swan-band, are enlarged. A ro-vibrational analysis and comparison with spectra of other injected species is outside the scope of this contribution, but can be found in detail in [3].

The deuterium spectrum of the Fulcher-band transition ($3p\ ^3\Pi_u \rightarrow 2s\ ^3\Sigma_g^+$) is depicted in fig. 4b. The main diagonal vibrational transitions ($v = v'$) up to $v = 5$ are indicated. The first main diagonal transition with $v = v' = 0$ is enlarged shown and the strongest Q lines (Q1-Q9) are marked. The rotational population of the excited state could be fitted according to a Boltzmann distribution with a rotational population temperature T_{rot} of about 1000 K which is in line with previous observations [4]. A more detailed analysis of the Fulcher-α band according to the methods described in [4] is topic of a forthcoming paper which will deal with the interpretation of the deuterium recycling flux and the molecular break-up [5] at the target plates of the helical divertor in TEXTOR [6].

5 Conclusion and outlook

The cross-dispersion spectrometer presented here is a good compromise to study spectroscopically the plasma boundary of fusion devices in the visible range, i.e the fuel recycling and the impurity sources. The system covers at once the spectral emission range between 372 nm and 680 nm with an almost constant resolving power of R=20000 over the full range. The dynamic range of 16 bit ensures the possibility of the simultaneous observation of atomic and molecular lines. The recommended integration time for the fibre-coupled system depends on the signal strength (extrinsic vs. intrinsic), but lays in the second range to ensure and optimised use of the dynamic range. Synergetic effects can be achieved when – like in TEXTOR – the system is embedded in a set of spectroscopic systems which complement one another [5]. The Mechelle provides the high
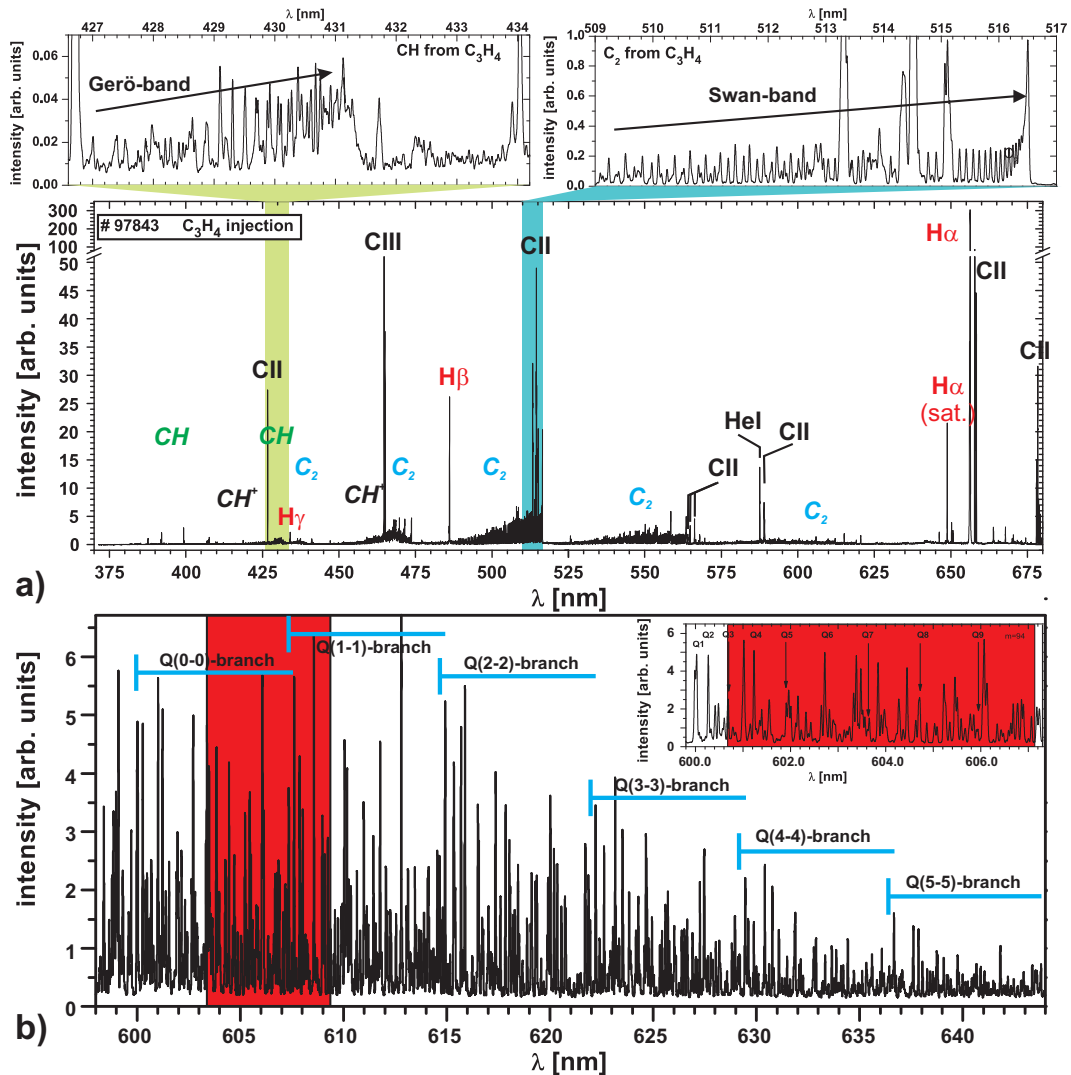
Fig. 4 a) C_3H_4 injection into the TEXTOR edge plasma through a gas injection module. The emission spectrum in the range between 372 nm and 680 nm recorded gap-free with the cross-dispersion spectrometer during the break-up of the injected hydrocarbon. The most important observable optical transitions of atomic and molecular break-up products are indicated. The *CH* Gerö band and the C_2 Swan band are highlighted and enlarged in separate figures on top of the "footprint" spectrum to demonstrate the good spectral resolution of the molecular bands. The integration time of the system was set to two seconds to ensure the complete coverage of the C_3H_4 injection pulse. b) The complete D_2 Fulcher-α band and the Q-lines of the first main diagonal transition. The spectral range in red indicates the coverage of the observation in the 94*th* order which is also highlighted in a separate box.

spectral resolution, the large wavelength coverage, and the high dynamic range, whereas the other systems with interference filters like photomultipliers or 2D CCD cameras provide the needed time and spatial resolution.

Experiments at TEXTOR provide "footprints" of the injected hydrocarbons C_3H_4 and information of D_2 molecules in the hot edge plasma. The appearance, the destruction path, the flux, the ratio, and the ro-vibrational population of the different species can now be studied in more detail within a single discharge.

Systems of the next generation of cross-dispersion spectrometers in prism /grating arrangement and equipped with prism, made of low absorption material with high dispersion, are currently developed to ensure a larger sensitivity in the spectral region below 450 nm. Such an opti-

mised system will be used for the observation of the new first wall and boundary layer at JET after installation of the new ITER-like wall with W and Be as plasma-facing material. The installation of an Echelle cross-dispersion spectrometer system is a also panned for the observation of the boundary layer in W7-X.

References

[1] S. Brezinsek et al., Physica Scripta **T111**, 42 (2004).
[2] P. Lindblom, Anal. Chim. Acta **380**, 353 (1999).
[3] S. Brezinsek et al., J. Nuclear Materials **313-316**, 967 (2003).
[4] S. Brezinsek et al.,J. Nuclear Materials **363-365**, 1119 (2007).
[5] S. Brezinsek et al., Plasma Phys. Control. Fusion **47**, 615 (2005)
[6] M. Lehnen et al., this conference